REPORT DOCUMENTATION PAGE

Form Approved OMB No. 0704-0188

1. REPORT DATE *(DD-MM-YYYY)*	2. REPORT TYPE	3. DATES COVERED *(From - To)*
	Technical Papers	

4. TITLE AND SUBTITLE

Please see attached

5a. CONTRACT NUMBER

5b. GRANT NUMBER

5c. PROGRAM ELEMENT NUMBER

6. AUTHOR(S)

5d. PROJECT NUMBER
2302

5e. TASK NUMBER
M1G2

5f. WORK UNIT NUMBER
346120

7. PERFORMING ORGANIZATION NAME(S) AND ADDRESS(ES)

Air Force Research Laboratory (AFMC)
AFRL/PRS
5 Pollux Drive
Edwards AFB CA 93524-7048

8. PERFORMING ORGANIZATION REPORT

9. SPONSORING / MONITORING AGENCY NAME(S) AND ADDRESS(ES)

Air Force Research Laboratory (AFMC)
AFRL/PRS
5 Pollux Drive
Edwards AFB CA 93524-7048

10. SPONSOR/MONITOR'S ACRONYM(S)

11. SPONSOR/MONITOR'S NUMBER(S)
Please see attached

12. DISTRIBUTION / AVAILABILITY STATEMENT

Approved for public release; distribution unlimited.

13. SUPPLEMENTARY NOTES

14. ABSTRACT

20030129 106

15. SUBJECT TERMS

16. SECURITY CLASSIFICATION OF:			17. LIMITATION OF ABSTRACT	18. NUMBER OF PAGES	19a. NAME OF RESPONSIBLE PERSON
					Leilani Richardson
a. REPORT	b. ABSTRACT	c. THIS PAGE	A		19b. TELEPHONE NUMBER *(include area code)*
Unclassified	Unclassified	Unclassified			(661) 275-5015

2300 M1G 2

MEMORANDUM FOR PRS (In-House/Contractor Publication)

FROM: PROI (STINFO) 08 Mar 2001

SUBJECT: Authorization for Release of Technical Information, Control Number: **AFRL-PR-ED-AB-2001-047**
Liu, C.T., "SIF Distribution in Cracked Photoelastic Rocket Motor Models; Preliminary Studies"

SEM Annual Conference on Experimental Mechanics **(Statement A)**
(Portland, OR, 4-6 Jun2001) (Deadline: 16 Mar 2001)

1. This request has been reviewed by the Foreign Disclosure Office for: a.) appropriateness of distribution statement, b.) military/national critical technology, c.) export controls or distribution restrictions, d.) appropriateness for release to a foreign nation, and e.) technical sensitivity and/or economic sensitivity.
Comments:_____

Signature _____ Date _____

2. This request has been reviewed by the Public Affairs Office for: a.) appropriateness for public release and/or b) possible higher headquarters review.
Comments: _____

Signature _____ Date _____

3. This request has been reviewed by the STINFO for: a.) changes if approved as amended, b) appropriateness of references, if applicable; and c.) format and completion of meeting clearance form if required
Comments:_____

Signature _____ Date _____

4. This request has been reviewed by PR for: a.) technical accuracy, b.) appropriateness for audience, c.) appropriateness of distribution statement, d.) technical sensitivity and economic sensitivity, e.) military/ national critical technology, and f.) data rights and patentability
Comments:_____

APPROVED/APPROVED AS AMENDED/DISAPPROVED

_____

PHILIP A. KESSEL Date
Technical Advisor
Space and Missile Propulsion Division

SIF Distributions In Cracked Photoelastic Rocket Motor Models; Preliminary Studies

C. W. Smith, D. M. Constantinescu and C. T. Liu*
Department of Engineering Science and Mechanics
Virginia Polytechnic Institute and State University
Blacksburg, VA 24061

Introduction

It is generally believed that motor grain design criteria which treats a part through crack in the fin of a rocket motor as an edge crack extending through the length of the motor is a conservative approach to the problem. Some estimates suggest a margin of safety of about 1.5 is achieved in doing so. In an attempt to improve cost effectiveness and efficiency, an experimental effort has been undertaken to obtain stress intensity factors (SIF)[s] at critical locations around the border of part through cracks in motor grain fins to compare with the design criteria using photoelastic models and a method of analysis developed by the first author [1] (Appendix A). The frozen stress photoelastic method is used and a new material employing amine type hardeners is used which may produce surface effects in the initial casting but appears far superior to other materials in other respects. Two-dimensional experimental studies at AFRL-Edwards AFB suggest that cracks tend to initiate at the locus along the fin tip, where the main tip radius coalesces with a much smaller corner radius. However, some manufacturers report cracks initiating on the axis of symmetry of the fin, possibly due to defects collected there during the casting process.

The following is a preliminary study to evaluate the new test material along a free surface and to check the stress fringe distribution along an uncracked fin tip for a scale model of an existing motor grain geometry.

The Experiments and Preliminary Results

To date three models have been tested and evaluated in order to address the above concerns. All models were the same shape and size (Fig. 1), and loaded with internal pressure combined with sufficient axial load to cancel the end face pressure.

Model 1 - This model was used solely to evaluate the fringe orders at the two critical locations around the fin tip. Fringe orders were measured along the paths indicated by the line of symmetry and a curve along the "squeezed" fringe regions (Fig. 2).

A boundary effect (black region) obscures the boundary points themselves and is found to be discolored in white light. Consequently, data had to be extrapolated to the boundary in order to obtain estimates of peak fringe orders. Fig. 3 shows the result and suggests that, in this case, the fringe order was slightly greater on the axis of symmetry of the fin than at the other critical point.

Model 2 - In this model, cracks were placed in two different fins, which were separated by an uncracked fin to eliminate interaction. The first crack was along the axis of symmetry of the fin and broke through to the outer wall at 0.145 MPa. In the second cracked fin, two cracks occurred of different lengths at the critical loci on either side of the axis of symmetry of the fin; the shorter one due to penetration of part of the device used to make the main crack. The shape of the longer crack showing how it turned during growth is shown in Fig. 4.

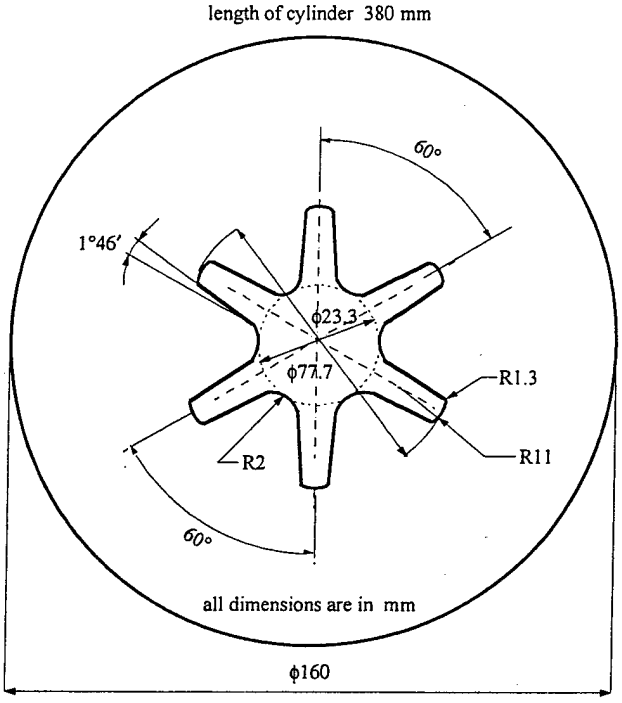

Fig 1: Model Geometry

SIF calculations were made on both sides of the crack surface, and consistent results were obtained at *A* in Fig. 4.

*AFRL/PRSM, 10 E. Saturn Blvd., Edwards AFB, CA 93524-7680

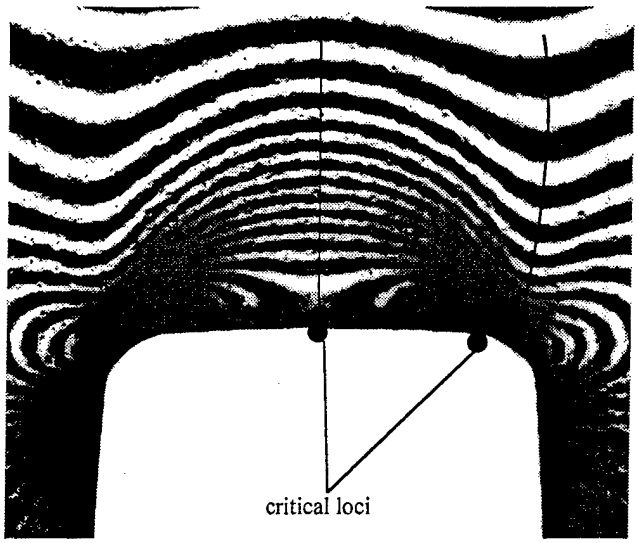

Fig 2: Fringe Pattern Near a Fin Tip In Uncracked Fin

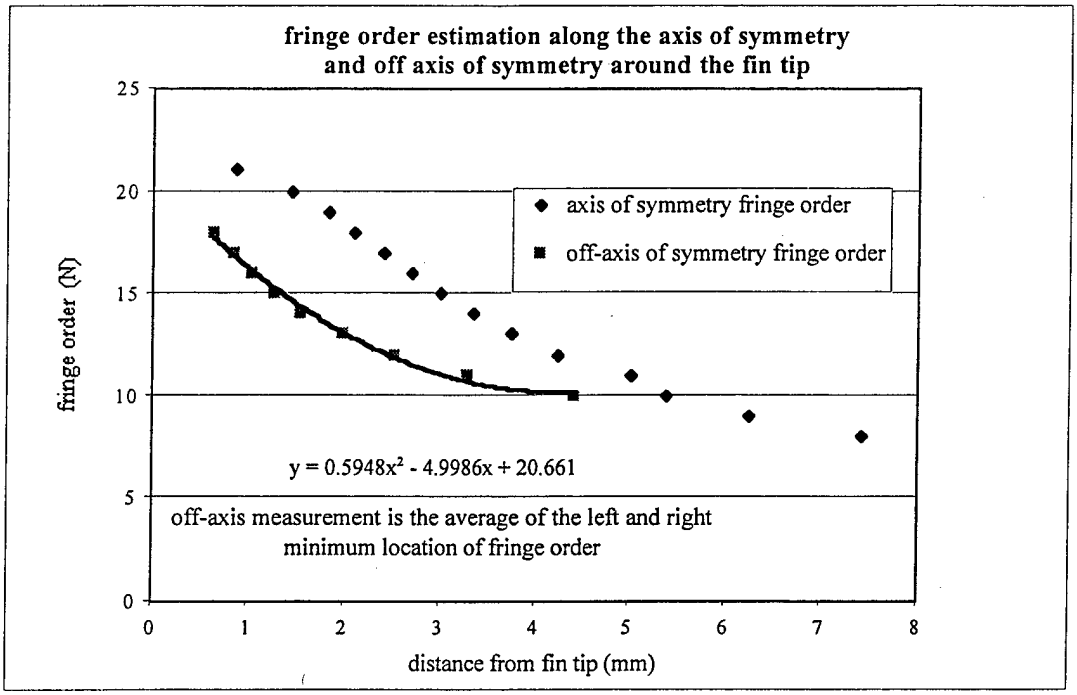

Fig 3: Fringe Orders at Critical Locations in Uncracked Fin

Results from the surfaces at C' and C'' were significantly larger but consistent (Table 1). Results for the shorter off-axis crack were determined only at maximum depth. Slices from the fin tip surface were used to evaluate the SIF values for the symmetric crack after breakthrough, but data were inconsistent and were discarded.

Model 3 - Symmetric cracks were driven into two fins separated by an uncracked fin. The longer crack began to grow at 0.103MPa, so the pressure was reduced to 0.048 MPa, stopping crack growth. After about 5 hrs., the growth started again in the longer crack and grew to the outer surface. The model was then stress frozen at 0.033 MPa. Consistent results were found in the short crack at both depth and surface and at the surface for the longer crack (Table 1).

Results from Models 2 and 3 are summarized in Table 1.

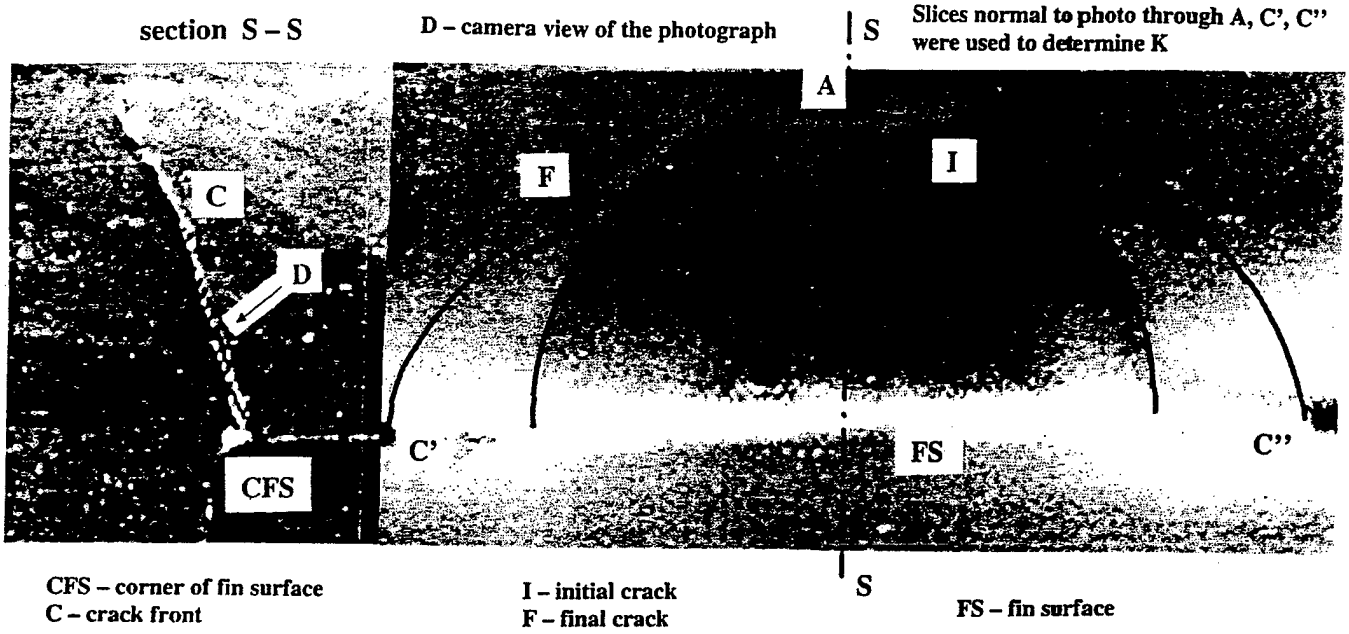

MF = 4.46

Fig 4: Shape of Off-Axis Crack After Growth

Discussion

From the preliminary tests described above, the following observations can be made:

i. It appears that the symmetric crack as well as the off-axis crack should be studied (Fig. 3).

ii. Some difficulty was encountered in obtaining consistent data for surface slices for penetrated symmetric cracks. Part of this difficulty may lie in leakage effects.

iii. Differences in the top and bottom surface slice results for non-penetrating cracks is partially due to their deviating from a perfect semi-ellipse in their shape, and there may also be a rind effect at the surface.

iv. Some end cap leakage occurred in Models 1 and 2. This was corrected by reinforcing the end caps with RTV glue.

Subsequent tests will employ the RTV end cap glue and substantially reduced axial load. Moreover, slices will not be taken directly in the fin surface but at an angle to it.

Acknowledgement

The authors gratefully acknowledge the support for the project under subcontract 98-522 with Sparta Inc. through AFRL.

Table 1

Load	Crack Description	$K\sqrt{\Phi}/p\sqrt{\pi a^+}$ + or c for surface crack		
		depth (d)	surface (s)	
			top	bottom
	Model 2			
P = 311.4 N p_{max} = 0.145 MPa p_{sf} = 0.07 MPa	Long off axis crack a/c = 0.66 a/t = 0.26	2.03	1.99	2.36
	Short off axis crack a/c = 1.26 a/t = 0.17	1.42		
	Long symmetric crack a/c = 0.9 a/t = 1.0	penetrated	disc.	disc.
	Model 3			
P = 311.4 N p_{max} = 0.103 MPa p_{sf} = 0.033 MPa	Short symmetric crack a/c = 0.5 a/t = 0.41	1.67	1.59	1.29
	Long symmetric crack a/c = 0.68 a/t = 1.0	penetrated	1.65	1.78
	$\Phi^* = 1 + 1.464\left(\frac{a}{c}\right)^{1.65}$ $\frac{a}{c} \le 1$ $\Phi^* = 1 + 1.464\left(\frac{c}{a}\right)^{1.65}$ $\frac{a}{c} > 1$	* Ref. [3] All flaws were characterized as semi-elliptic surface flaws of depth a and length $2c$		

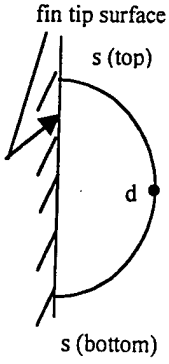

t = distance from fin tip to outer surface along axis of symmetry of fin

t = 37.08 mm

References

[1] Smith, C. W., and Kobayaski, A. S., "Experimental Fracture Mechanics" Chapter 20 of Handbook on Experimental Mechanics 2nd Revised ed. A. S. Kobayashi, Ed. Society for Experimental Mechanics VCH Publishers, 1993.

[2] Smith, C. W., "Experimental Method for Measuring Stress Intensity Factor Distributions in Three Dimensional Problems," Retrospective Ap. Mech. Rev. Vol. 53, No. 4, p R23-R32, April 2000.

[3] Raju, I. S. and Newman, J. C., Jr. "Stress Intensity Factors for Internal and External Surface Cracks in Cylindrical Vessels," ASME Journal of Pressure Vessel Technology, Vol. 104, pp. 293-298, Nov. 1982.

Appendix A (Mode I Algorithm)

Beginning with the Griffith-Irwin Equations, we may write, for Mode I, for the homogeneous case

$$\sigma_{ij} = \frac{K_I}{(2\pi r)^{1/2}} f_{ij}(\theta) + \sigma^o_{ij} \qquad (i, j = n, z) \qquad (1)$$

where: σ_{ij} are components of stress, K_I is SIF, r, θ are measured from crack tip (Fig. A-1), σ^o_{ij} are non-singular stress components. Then, along $\theta = \pi/2$, after truncating σ_{ij}

$$(\tau_{nz})_{max} = \frac{K_I}{(8\pi r)^{1/2}} + \tau^o = \frac{K_{AP}}{(8\pi r)^{1/2}} \qquad (2)$$

where $\tau^o = f(\sigma^o_{ij})$ and is constant over the data range, K_{AP}= apparent SIF, τ_{nz} = maximum shear stress in nz plane

$$\frac{K_{AP}}{\bar{\sigma}(\pi a)^{1/2}} = \frac{K_I}{\bar{\sigma}(\pi a)^{1/2}} + \frac{\sqrt{8}\tau^o}{\bar{\sigma}}\left(\frac{r}{a}\right)^{1/2} \qquad (3)$$

where (Fig. A-1) a = crack length, and $\bar{\sigma}$ = remote normal stress i.e.

$\frac{K_{AP}}{\bar{\sigma}(\pi a)^{1/2}}$ vs. $\sqrt{r/a}$ is linear.

Since from the Stress-Optic Law $(\tau_{nz})_{max} = nf/2t$ where, n = stress fringe order, f = material fringe value, t = specimen (or slice) thickness, then from Eq. 2,

$$K_{AP} = (8\pi r)^{1/2}(\tau_{nz})_{max} = (8\pi r)^{1/2} nf/2t$$

A typical plot of normalized K_{AP} vs. $\sqrt{r/a}$ for a homogeneous specimen is shown in Fig. A-2. For cases with additional near tip disturbances, a quadratic form of Eq. (3) may be indicated.

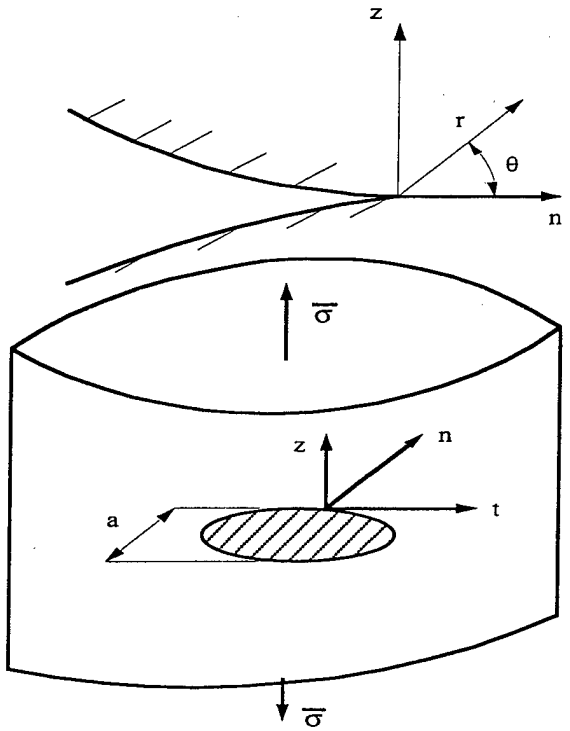

Fig A-1: Mode I Near-Tip Notation

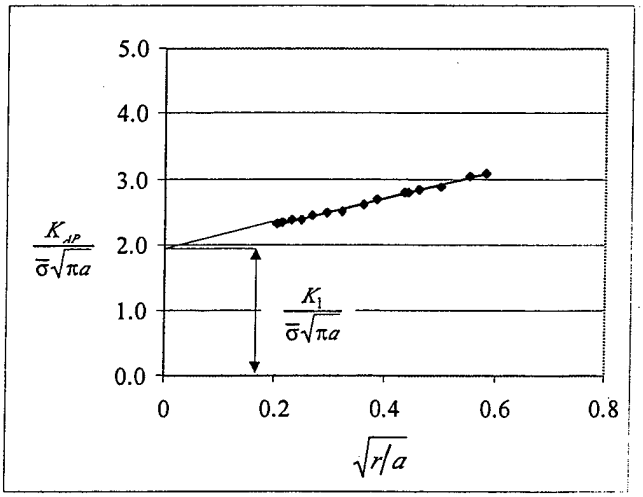

Fig A-2: Estimating Normalized SIF from Test Data